International Journal of Medical, Medicine and Health Sciences
ISSN: 2517-9969
Vol:11, No:5, 2017

Numerical Simulation of Bio-Chemical Diffusion in Bone Scaffolds

Masoud Madadelahi, Amir Shamloo, Seyedeh Sara Salehi

***Abstract*—**Previously, some materials like solid metals and their alloys have been used as implants in human's body. In order to amend fixation of these artificial hard human tissues, some porous structures have been introduced. In this way, tissues in vicinity of the porous structure can be attached more easily to the inserted implant. In particular, the porous bone scaffolds are useful since they can deliver important biomolecules like growth factors and proteins. This study focuses on the properties of the degradable porous hard tissues using a three-dimensional numerical Finite Element Method (FEM). The most important studied properties of these structures are diffusivity flux and concentration of different species like glucose, oxygen, and lactate. The process of cells migration into the scaffold is considered as a diffusion process, and related parameters are studied for different values of production/consumption rates.

***Keywords*—**Bone scaffolds, diffusivity, numerical simulation, tissue engineering.

I. Introduction

HEALING of bone defects is very important in clinical issues. Nowadays, synthetic bone replacement is used popularly for this purpose [1]. Bone scaffolds which are used in tissue engineering should be porous for at least two reasons [2]. The first reason is that vascularization and attachment of bone cells in three dimensions inside the scaffold will be occurred in a good condition. The recommended pores size for a perfect vascularization is diameter above 300 microns [3]. This range is reported between 100-400 micrometers in some literature studies [4], [5]. The second reason is that an appropriate porosity of the scaffolds can provide the conditions for seeding the cells easier and better. Besides, the porous scaffolds should not prevent the seeding cells from going to the neighbor tissues and should not promote the vascularization of the developing tissues [6]-[8].

There are different techniques for producing a porous degradable bone scaffold. One of these techniques is three-dimensional printing. This method has some advantages; first, the internal structure of the bone scaffold can be generated bases on the desired computer data. Second, the outer shape of the scaffold can be designed based on the patent's defect. For this purpose, MRI and CT scan of the target patient are used for gathering required data [3].

As it is mentioned, one of the advantages of porous degradable bone scaffolds is seeding the cells and delivering essential materials such as proteins and growth factors (for instance, transferring augmentation factor, bone morphological protein, and insulin like augmentation factor) [9]. Since the natural bones of human body are highly vascularized, it is desired for synthetic porous bone scaffolds to induce vascularization as soon as possible. Appropriate transportation of the nutrients, protein, and oxygen is very important in this process. Selard et al. presented a numerical simulation of nutrient diffusion in the intervertebral disc of human body [10]. They used a Finite Element Method (FEM) and built an axisymmetric two-dimensional numerical model.

Sanz-Herrera et al. presented a mathematical model on bone tissue regeneration in a specific family of bone scaffolds [11]. They concluded that velocity of the bone growth depends on the concentration of cells and mechanical stimulus inside the bone scaffold. This mechanical stimulus is an effective stress that regulates the formation of the bone.

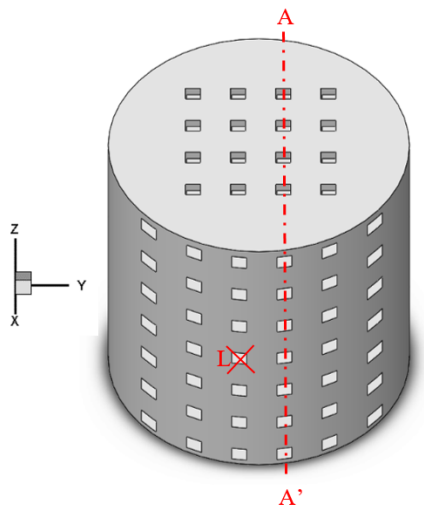

Fig. 1 A schematic view of a three-dimensional geometry for bone scaffold based on the work done by Leukers et al. [3]

In the present study, transport of the bio-molecules through the porous bone scaffolds and the consumption/production rate of the migrated cells inside porous bone scaffolds are investigated. This study does not pay attention to the mechanical properties of the scaffold and only focuses on the mass transport of fluid species inside the scaffold. It is assumed that three different kinds of species exist inside the fluid; oxygen, glucose, and lactate. These nutrients which are essential for cellular survival, diffuse from the blood around the tissue. In this way, different parameters such as mass

Masoud Madadelahi and S. S. Salehi are with Sharif University of Technology, Tehran, Islamic Republic of Iran.

Amir Shamloo is with the Sharif University of Technology, Tehran, Islamic Republic of Iran (corresponding author, phone: +98-21-66165691; fax: +98-21-66000021; e-mail: shamloo@sharif.edu).

diffusivity coefficient, concentration and production/ consumption rate of oxygen, glucose and lactate are extracted from the literature and imported to the numerical model. Fig. 1 depicts a bone scaffold which is designed based on the experimental work done by Leukers et al. [3]. As it is shown, the diameter of the scaffold is about 5 mm, and its height is considered 10 mm. Based on the experimental observations, pore size (length of the square-shaped pores) of this scaffold is considered about 500 micrometers.

II. Governing Equations

The concentration of species in the present study is calculated based on the mass-diffusion (1) [12].

$$\nabla.(-D\nabla C_i) = R_i \quad (1)$$

where C_i is the concentration of species i ($\frac{mol}{m^3}$), D is the mass diffusivity coefficient ($\frac{m^2}{s}$), and R_i is the production/consumption rate ($\frac{mol}{m^3 h}$). The index "i" varies from 1 to 3, corresponding to glucose, oxygen, and lactate, respectively. This equation is solved together with appropriate boundary conditions and initial conditions. These conditions include constant concentration on the boundaries which are in contact with the liquid solution with a specific amount of each species and zero-flux boundary condition (2) on all pore walls on which no mass-diffusion is possible.

$$n.(-D\nabla C_i) = 0 \quad (2)$$

where n is the normal vector on the surfaces on which the equation is applied as the boundary condition. Table I contains the constants which are extracted from the literature; the values of diffusivity coefficient, the production/consumption rate and concentration of glucose, oxygen and lactate [10]. As it is shown in Table I, maximum production/consumption rates are $-1\times10^{-9}\frac{mol}{mm^3 h}$, $-8.4\times10^{-9}\frac{mol}{mm^3 h}$, and $6.95\times10^{-11}\frac{mol}{mm^3 h}$ for glucose, oxygen, and lactate. These values are multiplied by a factor k which varies from 0 to 0.1.

III. Results and Discussion

All above mentioned equations and boundary conditions are solved using FEM (GMRES method) [13]. After grid independency check, a total number of 2923971 elements was selected in the numerical procedure. Fig. 2 displays the volumetric contour (mol/m^3) of glucose inside the pores of the bone scaffold with a k factor 0.1. Figs. 3 and 4 show the volumetric concentration contours (mol/m^3) of oxygen and lactic inside the scaffold. As it is seen, glucose and oxygen are consumed in the middle part of the scaffold and in vicinity of the walls of the scaffold, and the concentration of these two species increases. However, lactate which is produced by cells has a lower concentration in middle parts of the scaffold, and in vicinity of the walls, its concentration decreases due to leaving the scaffold.

TABLE I
Values of Constant Parameters Extracted from Literature

Symbol	Quantity	Value from literature
D_1	Mass Diffusion coefficient for Glucose	3.125×10^{-10} m^2/s
D_2	Mass Diffusion coefficient for Oxygen	1.056×10^{-9} m^2/s
D_3	Mass Diffusion coefficient for Lactate	5.486×10^{-10} m^2/s
C_1	Concentration of Glucose	4.75×10^{-9} mol/mm^3
C_2	Concentration of Oxygen	4.28×10^{-11} mol/mm^3
C_3	Concentration of Lactate	0.85×10^{-9} mol/mm^3
R_{max1}	Maximum consumption rate of Glucose	-1×10^{-9} mol/mm^3/h
R_{max2}	Maximum consumption rate of Oxygen	-8.4×10^{-9} mol/mm^3/h
R_{max3}	Maximum production rate of Lactate	6.95×10^{-11} mol/mm^3/h

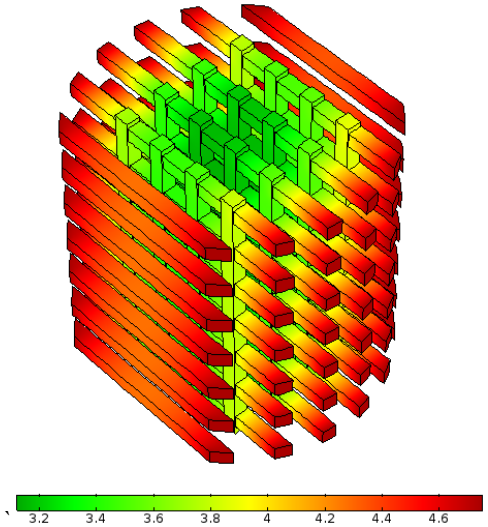

Fig. 2 Volumetric contour of concentration of the glucose (mol/m^3) with "k=0.1"

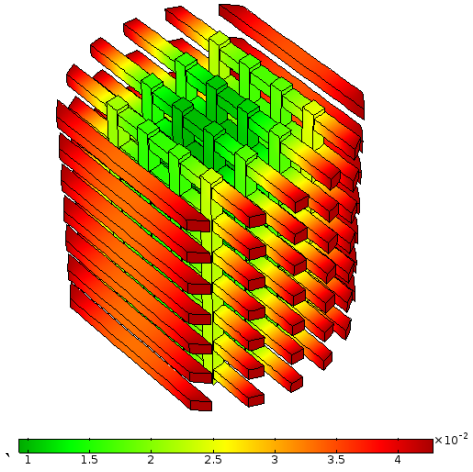

Fig. 3 Volumetric contour of concentration of the oxygen (mol/m^3) with "k=0.1"

Figs. 5-7 depict the magnitude and vector plot of diffusion flux of glucose, oxygen, and lactic, respectively. These figures are produced on the section AA' (Fig. 1) with a factor "k=0.1". According to these figures, the diffusion flux of

glucose and oxygen decreases inside the scaffold and has an inward direction. However, for lactate which is produced inside the scaffold, the diffusion flux increases in middle parts and has an outward direction.

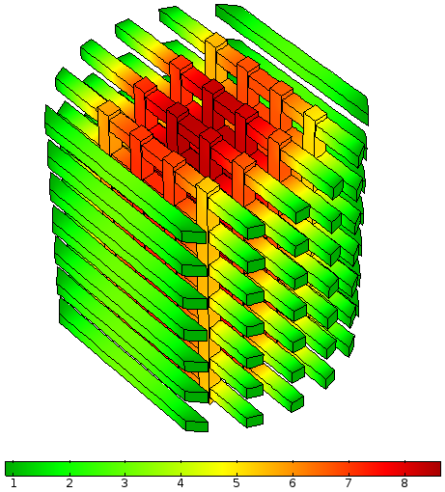

Fig. 4 Volumetric contour of concentration of the lactate (mol/m^3) with "k=0.1"

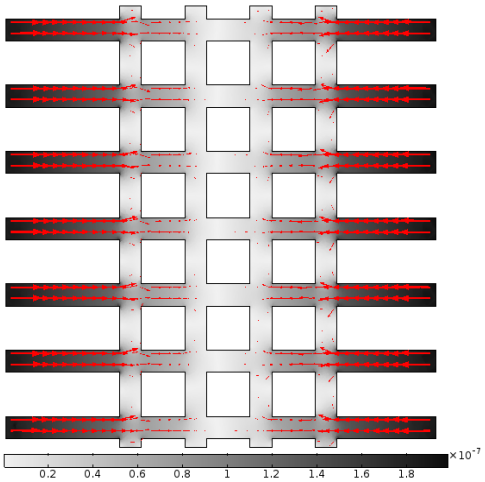

Fig. 5 Magnitude and vector plot of diffusion flux of glucose in the vertical cross section AA'

Figs. 8-10 show concentration profiles along the point "L" (x-direction in Fig. 1). The production/reaction rate is changed by dimensionless factor k which varies from 0 to 0.1. As it is seen, the concentration inside the bone scaffold decreases for glucose and oxygen, and for values of "k" greater than 0.1, the amount of oxygen decreases and becomes negative which is impossible. This means that the oxygen is limiting factor for cells metabolism. However, for lactate, the concentration has a maximum in the middle of the scaffold and goes down in near-wall regions.

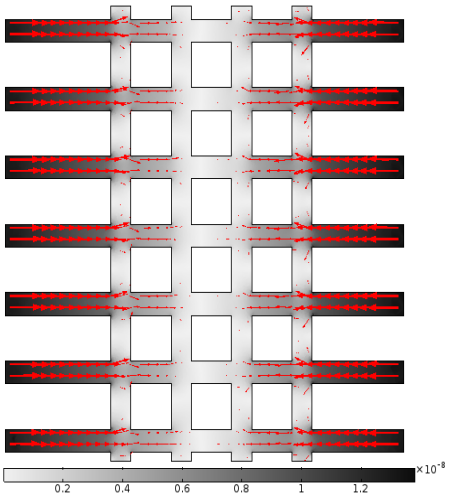

Fig. 6 Magnitude and vector plot of diffusion flux of oxygen in the vertical cross section AA'

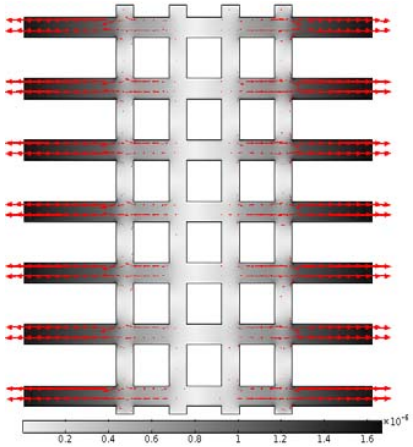

Fig. 7 Magnitude and vector plot of diffusion flux of lactate in the vertical cross section AA'

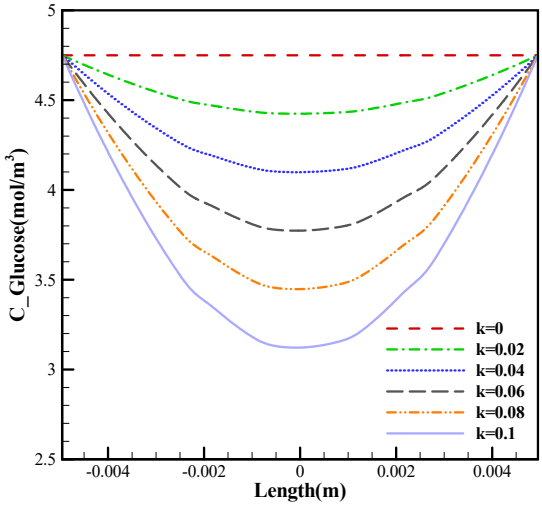

Fig. 8 Volumetric contour of concentration of the glucose (mol/m^3) along line L

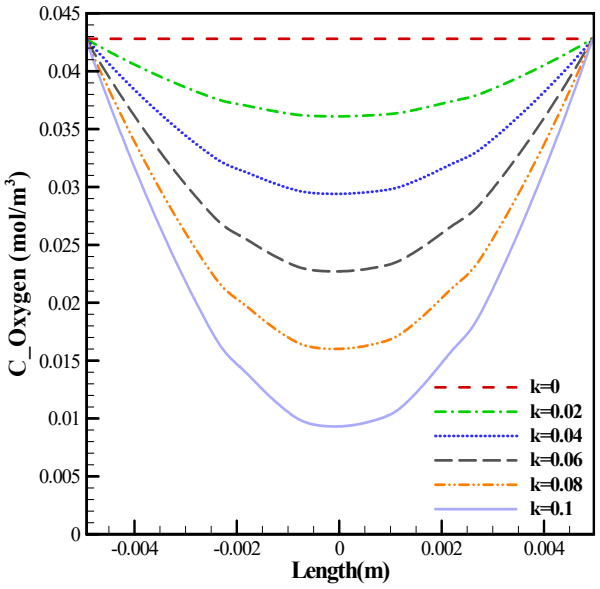

Fig. 9 Volumetric contour of concentration of the oxygen (mol/m^3) along line L

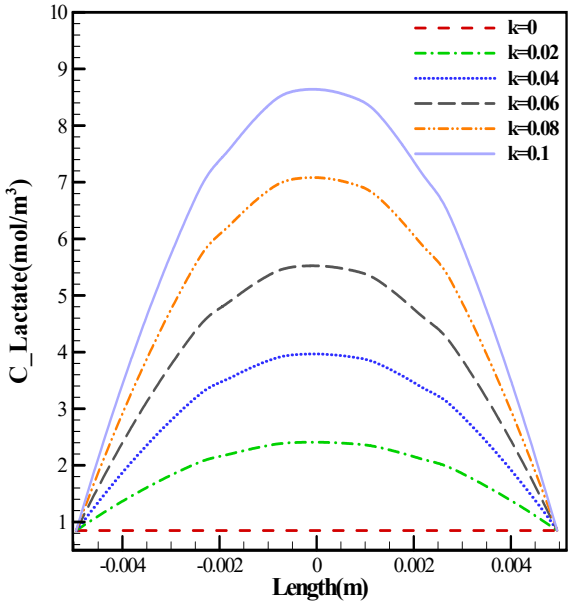

Fig. 10 Volumetric contour of concentration of the lactate (mol/m^3) along line L

REFERENCES

[1] Tadic, D. and M. Epple, A thorough physicochemical characterisation of 14 calcium phosphate-based bone substitution materials in comparison to natural bone. Biomaterials, 2004. 25(6): p. 987-994.
[2] Lei, Y., et al., Strontium hydroxyapatite/chitosan nanohybrid scaffolds with enhanced osteoinductivity for bone tissue engineering. Materials Science and Engineering: C, 2017. 72: p. 134-142.
[3] Leukers, B., et al., Hydroxyapatite scaffolds for bone tissue engineering made by 3D printing. Journal of Materials Science: Materials in Medicine, 2005. 16(12): p. 1121-1124.
[4] Ostrowska, B., et al., Influence of internal pore architecture on biological and mechanical properties of three-dimensional fiber deposited scaffolds for bone regeneration. Journal of Biomedical Materials Research Part A, 2016.
[5] Chang, B., et al., Influence of pore size of porous titanium fabricated by vacuum diffusion bonding of titanium meshes on cell penetration and bone ingrowth. Acta biomaterialia, 2016. 33: p. 311-321.
[6] Wintermantel, E., et al., Tissue engineering scaffolds using superstructures. Biomaterials, 1996. 17(2): p. 83-91.
[7] Mikos, A.G., et al., Laminated three-dimensional biodegradable foams for use in tissue engineering. Biomaterials, 1993. 14(5): p. 323-330.
[8] Kang, H.-W., Y. Tabata, and Y. Ikada, Fabrication of porous gelatin scaffolds for tissue engineering. Biomaterials, 1999. 20(14): p. 1339-1344.
[9] Sohail, A., et al., Numerical Modelling of Effective Diffusivity in Bone Tissue Engineering. World Academy of Science, Engineering and Technology, International Journal of Medical, Health, Biomedical, Bioengineering and Pharmaceutical Engineering, 2015. 9(1): p. 82-86.
[10] Sélard, É., A. Shirazi-Adl, and J.P. Urban, Finite element study of nutrient diffusion in the human intervertebral disc. Spine, 2003. 28(17): p. 1945-1953.
[11] Sanz-Herrera, J., J. Garcia-Aznar, and M. Doblare, A mathematical model for bone tissue regeneration inside a specific type of scaffold. Biomechanics and modeling in mechanobiology, 2008. 7(5): p. 355-366.
[12] Bird, R.B., W.E. Stewart, and E.N. Lightfoot, Transport Phenomena John Wiley & Sons. New York, 1960: p. 413.
[13] Saad, Y., Iterative methods for sparse linear systems. 2003: Siam.